Influence of nozzle cavity on indirect vortex- and entropy-sound production

Hirschberg, L.; Hulshoff, S. J.; Collinet, J.; Schram, C.; Schuller, T.

DOI
10.2514/1.J058138

Publication date
2019

Document Version
Final published version

Published in
AIAA Journal

AIAA JOURNAL
Vol. 57, No. 7, July 2019

Technical Notes

Influence of Nozzle Cavity on Indirect Vortex- and Entropy-Sound Production

L. Hirschberg*
von Kármán Institute for Fluid Dynamics, 1640 Sint-Genesius-Rode, Belgium
S. J. Hulshoff†
Delft University of Technology, 2629 HS Delft, The Netherlands
J. Collinet‡
ArianeGroup, 78130 Les Mureaux, France
C. Schram§
von Kármán Institute for Fluid Dynamics, 1640 Sint-Genesius-Rode, Belgium
and
T. Schuller§
Institute of Fluid Mechanics of Toulouse, 31400 Toulouse, France

DOI: 10.2514/1.J058138

Nomenclature

B'	=	total enthalpy fluctuation, $m^2 \cdot s^{-2}$
c	=	local speed of sound, $m \cdot s^{-1}$
E_T	=	total energy density, $J \cdot m^{-3}$
e	=	specific energy, $J \cdot kg^{-1}$
$\boldsymbol{F}_E$	=	external momentum source, $N \cdot kg^{-1}$
$\boldsymbol{f}$	=	force density, $N \cdot m^{-3}$
$\boldsymbol{f}_s$	=	force density in case of entropy sound, $N \cdot m^{-3}$
$\boldsymbol{f}_v$	=	force density in case of vortex sound, $N \cdot m^{-3}$
G	=	Green's function, $m^{-1} \cdot s^{-1}$
G_c	=	acoustic flow generated by compression of the fluid around the nozzle inlet, $m^{-1} \cdot s^{-1}$
G_r	=	acoustic flow due to radiation through the nozzle, $m^{-1} \cdot s^{-1}$
p'/p	=	relative pulsation amplitude
Q_E	=	energy source term, $J \cdot m^{-3} \cdot s^{-1}$
R_s	=	entropy-spot-core radius, m
R_Γ	=	vortex-core radius, m
S_1	=	upstream channel height measured with respect to the symmetry axis, m
S_2	=	nozzle throat height, m
t	=	time, s
t_{burn}	=	duration of a LP9 subscale-model experiment, s
U	=	average upstream flow speed, $m \cdot s^{-1}$
$\boldsymbol{U}$	=	average upstream flow velocity, $m \cdot s^{-1}$
V_c	=	nozzle cavity volume, m^3
$\boldsymbol{v}$	=	local velocity, $m \cdot s^{-1}$
Γ	=	vortex circulation, $m^2 \cdot s$
$\tilde{\Gamma}$	=	dimensionless vortex circulation, $\Gamma/(US_1)$
$\delta\rho$	=	density difference between the entropy spot and surrounding homentropic flow, $kg \cdot m^{-3}$
ρ	=	density of upstream homentropic flow, $kg \cdot m^{-3}$
$\boldsymbol{\omega}$	=	vorticity; $\nabla \times \boldsymbol{v}$, s^{-1}
∇	=	gradient operator, m^{-1}

Received 26 November 2018; revision received 15 February 2019; accepted for publication 17 February 2019; published online 14 March 2019.

*Ph.D. Student; also ArianeGroup, 78130 Les Mureaux, France; CentraleSupélec, 91192 Gif-sur-Yvette, France; lionel.hirschberg@vki.ac.be. Student Member AIAA.
†Assistant Professor, Faculty of Aerospace Engineering.
‡Engineer.
§Professor.

I. Introduction

In LARGE solid rocket motors (SRMs) operating in the moderate-amplitude regime $p'/p = \mathcal{O}(10^{-3})$ [1,2], vortex-driven indirect sound leads to the establishment of a feedback loop resulting in self-sustained pressure pulsations [1,3–8]. Integral to this mechanism is the interaction of vortices, created near a geometric feature of the combustion chamber, with the nozzle as they exit (vortex-nozzle interaction) [1,4,6,8–10]. Another possible (but in the context of SRMs) overlooked mechanism is the interaction of density inhomogeneities, created by nonuniform combustion, with the nozzle as they exit (entropy-spot-nozzle interaction). Entropy sound as a source of sustained pressure pulsations is a well-documented problem in aircraft turbine engines [11,12]. In the context of SRMs, for both vortex-nozzle and entropy-spot-nozzle interaction, a traveling acoustic wave is produced that, after reflection, can interact with the flow to produce additional vortices or entropy spots. The result is a feedback loop that sustains the oscillation.

For vortex-driven self-sustained pressure pulsations, the presence of a cavity around the nozzle inlet (as in integrated nozzles) has been demonstrated to have a major influence [1,4,6,7]. Indeed, cold-gas scale experiments of a scale model of the Ariane 5 SRM show that the limit-cycle amplitude of vortex-driven self-sustained pressure pulsations is proportional to the nozzle cavity volume [6]. The importance of this cavity volume V_c for vortex-driven pulsations was analyzed in Refs. [1,2,8]. The cavity appears after partial combustion of the propellant surrounding the inlet of the integrated nozzle used in most SRMs.

In this technical Note, the influence of a nozzle cavity surrounding the nozzle inlet on upstream indirect entropy-sound radiation is reported for the first time. A qualitative explanation of the results is provided in Sec. III. The results are also used to offer a new interpretation of LP9 subscale-model experiments with the combustion of non-metalized propellant [7].

II. Comparison of Vortex-Nozzle and Entropy-Spot-Nozzle Induced Indirect Sound

Systematic studies of vortex-nozzle and entropy-spot-nozzle interactions have been carried out using a two-dimensional Euler internal aeroacoustics code [2,10], which solves the compressible frictionless governing (Euler) equations:

$$\frac{\partial \rho}{\partial t} + \nabla \cdot (\rho \boldsymbol{v}) = 0 \tag{1}$$

$$\frac{\partial \rho \boldsymbol{v}}{\partial t} + \nabla \cdot (\rho \boldsymbol{v}\boldsymbol{v} + p\mathbf{1}) = \rho \boldsymbol{F}_E \tag{2}$$

$$\frac{\partial E_T}{\partial t} + \nabla \cdot ((E_T + p)\boldsymbol{v}) = Q_E \tag{3}$$

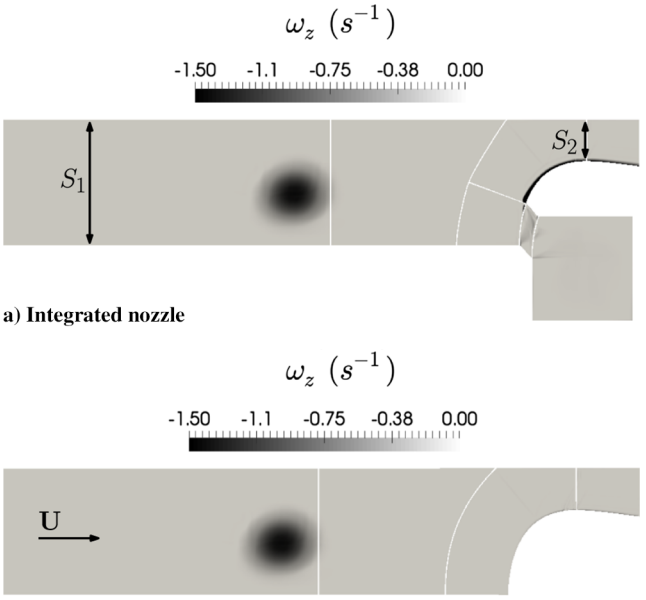

Fig. 1 Nozzle inlet geometries for a nozzle inlet Mach number of $M = 0.197$ a) with and b) without a nozzle cavity. The grayscale is for the normal vorticity component ω_z.

where $E_T = \rho(e + \boldsymbol{v}^2/2)$ is the total energy density, $\rho \boldsymbol{F}_E$ is an external momentum source density, and Q_E is an external energy source. For the simulations considered here, the external momentum source $\boldsymbol{F}_E$ was used to generate vortices, whereas the energy source term Q_E was used to generate entropy spots. The ideal gas law with a constant heat capacity ratio of 1.4 was used as an equation of state. The simulations were initialized with choked steady flow solutions on nozzle domains with contraction ratios of S_1/S_2 (Fig. 1a) corresponding to the desired upstream Mach number M. Only the lower half of the problem was simulated using a symmetry condition on the upper boundary of the numerical domain. At the walls, a zero normal velocity $\boldsymbol{v} \cdot \boldsymbol{n} = 0$ condition was applied. Nonreflecting boundary conditions were used on both the inflow and outflow boundaries. Note that, for the choked cases considered, information could not travel back upstream through the sonic line; thus, the choice of outflow boundary condition was noncritical. In Ref. [2], a detailed description of the numerical approach and the method for the generation of vortices and entropy spots used for this study can be found. For the current study, either a vortex of core radius R_Γ and circulation Γ or a circular entropy spot of radius R_s equal to the vortex radius $R_s = R_\Gamma = 0.3S_1$ and density difference $\delta\rho$ with respect to its surroundings was generated upstream of the choked nozzle. In both cases, generation was started at a longitudinal distance of $6.5S_1$ upstream of the nozzle inlet. The $\boldsymbol{F}_E$ or Q_E field was moved with the emerging structure for a longitudinal distance of approximately $4S_1$; after which, $\boldsymbol{F}_E$ or Q_E were set to zero. The mature structures were then allowed to travel downstream and exit through the nozzle to produce an upstream-traveling acoustic pulse. The upstream release height h measured from the lower upstream channel wall to the center of the structure was varied in the range of $0.4 \leq h/S_1 \leq 0.6$.

The simulations were conducted with a second-order total-variation-diminishing scheme with Roe's approximate Riemann solver [10,13]. Time marching was performed using a five-stage Runge–Kutta method [13]. Simulations with 36, 54, and 81 grid points per vortex-core radius R_Γ or entropy-spot R_s were carried out. The results were used to determine the observed order of accuracy, which was found to be 1.8 with an associated discretization error of 1% on the 36 grid points per core radius mesh. Thus, 36 points per core radius grids were used for the remaining simulations. A numerical pressure probe was placed, at a distance $7.25S_1$ upstream from the nozzle inlet, in order to record the resulting upstream-traveling acoustic wave.

Two nozzle inlet geometries were considered. Figure 1a shows the first, which is an integrated nozzle geometry with a cavity surrounding its inlet. Figure 1b shows the second, which is a nozzle with the inlet forming a right-angle corner with the combustion chamber sidewall. The vorticity distribution field and the approaching vortex upstream from the nozzle are shown: both for the cases with a nozzle cavity (Fig. 1a) and without a nozzle cavity (Fig. 1b). One observes a thin layer of vorticity that develops from the sharp leading edge of the nozzle cavity inlet. Its presence does not contribute to the production of sound. The cavity volume V_c chosen for the integrated nozzle simulations corresponds to the volume of an upstream duct segment of length $0.7S_1$. This volume is defined as the difference in volume between the configuration in Figs. 1a and 1b, respectively. For the simulations discussed here, V_c corresponds to that of nozzle 2 in the cold-gas experiments of Anthoine [1,4] and is, at a reduced scale, representative of the nozzle cavity volume of an Ariane 5 SRM [4].

Simulations were carried out for upstream Mach numbers within the range $0.05 \leq M \leq 0.2$, which is a range typical for SRMS [4]. For the simulations shown in Fig. 2, an upstream Mach number of $M \equiv U/c = 0.053$ was used, where U is the uniform upstream flow velocity and c is the upstream local speed of sound. The entropy-spot-nozzle interaction simulations were carried out with $\delta\rho/\rho = -0.03$. To obtain the results for the vortex-nozzle interaction shown in Fig. 2b, a dimensionless vortex circulation of $\tilde{\Gamma} \equiv \Gamma/(US_1) = -0.9$ was used. The minus sign is due to the fact that the lower part of a vortex pair was simulated, and the flow direction was from left to right. In a SRM, vortices are generated by the concentration of negative vorticity originally present in the lower part of the flow [1,4,6]. The chosen circulation magnitude of $|\tilde{\Gamma}| = 0.9$ is in the range of vortex circulation expected in SRMs [8]: $0.1 < |\tilde{\Gamma}| < 1$.

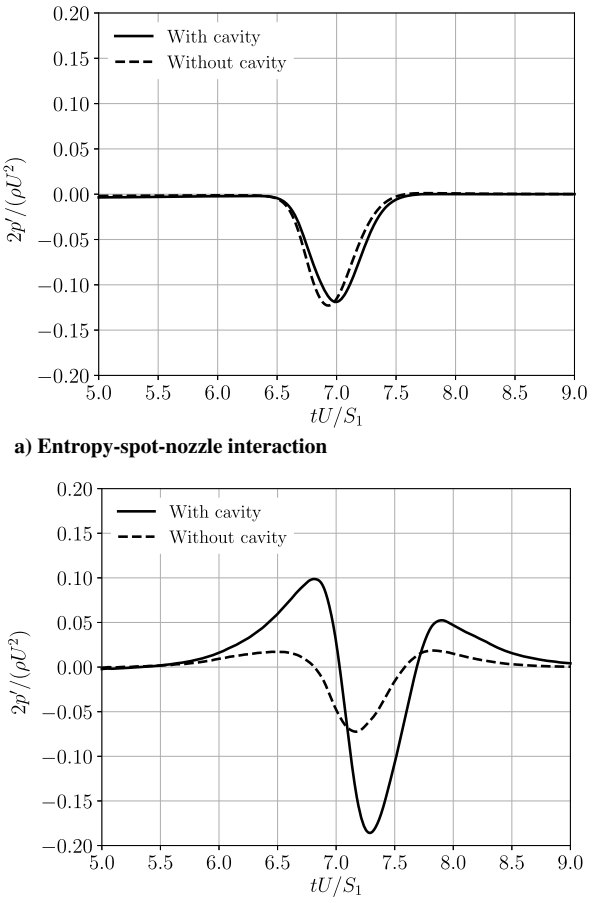

Fig. 2 Upstream acoustic response, with and without nozzle cavity, due to a) entropy-spot-nozzle and b) vortex-nozzle interactions.

In Fig. 2, the acoustic responses for both geometries are shown, scaled by the mean upstream dynamic pressure $\rho U^2/2$. Time is nondimensionalized as tU/S_1, where S_1 is the upstream channel height. Note that the entropy-spot-nozzle interaction is marginally affected by the presence of the cavity in Fig. 2a. This was also found for a range of values of the density inhomogeneity of $-0.12 \leq \delta\rho/\rho \leq -0.03$, upstream Mach numbers of $0.053 \leq M \leq 0.197$, and entropy-spot-core radii of $0.2 \leq R_s/S_1 \leq 0.4$. In contrast, one observes in Fig. 2b that the vortex-nozzle interaction pulse amplitude is increased by a factor three in the presence of the nozzle cavity. The pulse shape is also modified by the presence of the cavity.

III. Discussion

Using an aeroacoustic analogy with as its natural aeroacoustic variable B' (the total enthalpy fluctuation), both entropy-spot-nozzle and vortex-nozzle sound production can be qualitatively understood as a force density field $\boldsymbol{f}$ acting on the acoustic field [2,14]. The integral form of the analogy is [2,9]

$$B' = -\int_{-\infty}^{\infty}\int_{V}\frac{\boldsymbol{f}}{\rho}\cdot\nabla G\,\mathrm{d}^3y\,\mathrm{d}\tau \tag{4}$$

with $G = G(\boldsymbol{x}, \boldsymbol{y}, t-\tau)$ as the tailored Green's function (viz., the acoustic response due to a point source generated unit pulse) located at $\boldsymbol{x} = \boldsymbol{y}$ and activated at $t = \tau$. In the case of entropy sound, the force density is $\boldsymbol{f}_s = \delta\rho\mathrm{D}\boldsymbol{v}/\mathrm{D}t$ [14]; whereas for vortex sound, the force field is $\boldsymbol{f}_v = -\rho(\boldsymbol{\omega}\times\boldsymbol{v})$ [1,8], where ρ is the fluid density, $\boldsymbol{v}$ is the local flow velocity, and $\boldsymbol{\omega} \equiv \nabla\times\boldsymbol{v}$ is the vorticity. The gradient of the Green's function ∇G has two components. The first ∇G_r is the acoustic flow due to radiation through the nozzle that, in the first approximation, is parallel to the flow velocity $\boldsymbol{v}$ along the path of the vortex or entropy spot. The second ∇G_c is the acoustic flow generated by compression of the fluid around the nozzle inlet. This acoustic flow ∇G_c is, in the first-order approximation, normal to $\boldsymbol{v}$ along the path of the vortex and entropy spot [1,6,8]. Consequently, $\boldsymbol{f}_v$, which is normal to $\boldsymbol{v}$, mostly radiates noise thanks to the compressibility component ∇G_c in the presence of the nozzle cavity. This effect appears to be important, as shown in Fig. 2b. The normal component of $\boldsymbol{f}_s$ aligned with ∇G_c is due to centrifugal acceleration. This effect appears to be negligible (Fig. 2a). The added compressibility due to the nozzle cavity does not significantly affect the acoustic radiation caused by the entropy spot. Furthermore, it has been verified that, in the region in which sound is produced, the convective acceleration is dominated by the acceleration along the streamline. The acceleration normal to the streamline is reduced due to the presence of an inflection point in the trajectory.

It is striking that, in the LP9 subscale-model experiments with the combustion of nonmetalized propellant reported by Gallier et al. [7], the self-sustained pressure pulsation amplitude increases by an order of magnitude in the presence of a nozzle cavity as shown in Fig. 3.

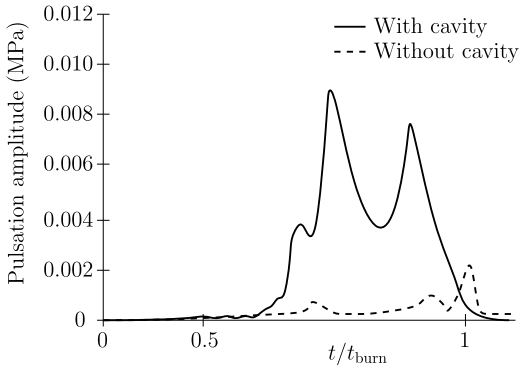

Fig. 3 LP9 subscale experiments with combustion, with and without a nozzle cavity, from Ref. [7]. Here, t_{burn} is the duration of a firing, and $t/t_{\mathrm{burn}} = 1$ when all propellant has been depleted.

The present results demonstrate that the addition of a cavity strongly enhances vortex-sound production, but it does not affect entropy-sound production. One can thus infer that, for the LP9 experiments with a cavity, indirect sound sources are dominated by vortex-nozzle interaction, and entropy sound is likely to be negligible.

IV. Conclusions

Simulation results have been presented that suggest that, in contrast to vortex-nozzle interaction, entropy-spot-nozzle interaction is not significantly influenced by the presence of a nozzle cavity. This result is used to give a new qualitative interpretation of LP9 subscale-model experiments with the combustion of nonmetalized propellant. It is inferred that vortex-sound production dominates, due to the strong amplification of the limit-cycle pulsation amplitude in these experiments in the presence of a nozzle cavity.

Acknowledgments

This work was funded by Association Nationale Recherche et de la Technologie (ANRT) and ArianeGroup through a Conventions Industrielles de Formation par la REcherche (CIFRE) grant (no. 2015/0938). Support offered by Serge Radulovic and Franck Godfroy of ArianeGroup is acknowledged.

References

[1] Hirschberg, L., Schuller, T., Collinet, J., Schram, C., and Hirschberg, A., "Analytical Model for the Prediction of Pulsations in a Cold-Gas Scale-Model of a Solid Rocket Motor," *Journal of Sound and Vibration*, Vol. 19, April 2018, pp. 445–368. doi:10.1016/j.jsv.2018.01.025

[2] Hirschberg, L., "Low Order Modeling of Vortex Driven Self-Sustained Pressure Pulsations in Solid Rocket Motors," Ph.D. Thesis, CentraleSupélec, Univ. Paris Saclay, France, 2019.

[3] Dotson, K. W., Koshigoe, S., and Pace, K. K., "Vortex Shedding in a Large Solid Rocket Motor Without Inhibitors at the Segmented Interfaces," *Journal of Propulsion and Power*, Vol. 13, No. 2, 1997, pp. 197–206. doi:10.2514/2.5170

[4] Anthoine, J., "Experimental and Numerical Study of Aeroacoustic Phenomena in Large Solid Propellant Boosters, with Application to the Ariane 5 Solid Rocket Motor," Ph.D. Thesis, Free Univ. of Brussels, Brussels, 2000.

[5] Fabignon, Y., Dupays, J., Avalon, G., Vuillot, F., Lupoglazoff, N., Casalis, G., and Prévost, M., "Instabilities and Pressure Oscillations in Solid Rocket Motors," *Aerospace Science and Technology*, Vol. 7, No. 3, 2003, pp. 191–200. doi:10.1016/S1270-9638(02)01194-X

[6] Anthoine, J., Buchlin, J.-M., and Hirschberg, A., "Effect of Nozzle Cavity on Resonance in Large SRM: Theoretical Modeling," *Journal of Propulsion and Power*, Vol. 18, No. 2, 2002, pp. 304–311. doi:10.2514/2.5935

[7] Gallier, S., Prevost, M., and Hijlkema, J., "Effects of Cavity on Thrust Oscillations in Subscale Solid Rocket Motors," *45th AIAA/ASME/ASEE Joint Propulsion Conference & Exhibit*, AIAA Paper 2009-5253, Aug. 2009. doi:10.2514/6.2009-5253

[8] Hirschberg, L., Hulshoff, S. J., Collinet, J., Schram, C., and Schuller, T., "Vortex Nozzle Interaction in Solid Rocket Motors: A Scaling Law for Upstream Acoustic Response," *Journal of the Acoustical Society of America*, Vol. 144, No. 1, 2018, pp. EL46–EL51. doi:10.1121/1.5046441

[9] Hirschberg, L., Schuller, T., Schram, C., Collinet, J., Yiao, M., and Hirschberg, A., "Interaction of a Vortex with a Contraction in a 2-Dimensional Channel: Incompressible Flow Prediction of Sound Pulse," *23rd AIAA/CEAS Aeroacoustics Conference*, AIAA Paper 2017-3701, 2017. doi:10.2514/6.2017-3701

[10] Hulshoff, S. J., Hirschberg, A., and Hofmans, G. C. J., "Sound Production of Vortex Nozzle Interactions," *Journal of Fluid Mechanics*, Vol. 439, July 2001, pp. 335–352. doi:10.1017/S0022112001004554

[11] Dowling, A. P., and Mahmoudi, Y., "Combustion Noise," *Proceedings of the Combustion Institute*, Vol. 35, No. 1, 2015, pp. 65–100. doi:10.1016/j.proci.2014.08.016

[12] Morgans, A. S., and Duran, I., "Entropy Noise: A Review of Theory, Progress and Challenges," *International Journal of Spray and Combustion Dynamics*, Vol. 8, No. 4, 2016, pp. 285–298. doi:10.1177/1756827716651791

[13] Venkatakrishnan, V., and Jameson, A., "Computation of Unsteady Transonic Flows by the Solution of Euler Equations," *AIAA Journal*, Vol. 26, No. 8, 1988, pp. 974–981. doi:10.2514/3.9999

[14] Howe, M. S., "Contributions to the Theory of Aerodynamic Sound: with Applications to Excess Jet Noise and the Theory of the Flute," *Journal of Fluid Mechanics*, Vol. 71, No. 4, 1975, pp. 625–673. doi:10.1017/S0022112075002777

L. Ukeiley
Associate Editor